Energy Research and Development Division FINAL PROJECT REPORT

PRODUCTION OF AN OPERATING PHOTOVOLTAIC SUBMODULE FOR INTEGRATION INTO A HIGH-EFFICIENCY CONVERSION UNIT

Prepared for: California Energy Commission

Prepared by: United Innovations, Inc.

JULY 2011

CEC-500-2013-096

Prepared by:

Primary Author(s):

Ugur Ortabasi

United Innovations, Inc. 1680 Meadowglen Lane Encinitas, CA 92024 (760) 632-6693

Contract Number: 500-09-011

Prepared for:

California Energy Commission

Matt Coldwell Contract Manager

Fernando Pina
Office Manager
Energy Systems Research Office

Laurie ten Hope

Deputy Director

ENERGY RESEARCH AND DEVELOPMENT DIVISION

Robert P. Oglesby Executive Director

DISCLAIMER

This report was prepared as the result of work sponsored by the California Energy Commission. It does not necessarily represent the views of the Energy Commission, its employees or the State of California. The Energy Commission, the State of California, its employees, contractors and subcontractors make no warrant, express or implied, and assume no legal liability for the information in this report; nor does any party represent that the uses of this information will not infringe upon privately owned rights. This report has not been approved or disapproved by the California Energy Commission nor has the California Energy Commission passed upon the accuracy or adequacy of the information in this report.

ACKNOWLEDGEMENTS

This work has been supported by the California Energy Commission through the Public Interest Energy Research Energy Innovations Small Grant Program (PIER EISG). The author acknowledges the outstanding guidance provided by Matt Coldwell, California Energy Commission contract manager, and Dr. John Crockett, coordinator, EISG Technology Transfer Program. The author expresses his most sincere gratitude to Dr. Gerald Braun, Energy Commission Energy Generation, Research Office, Renewables, Team Lead, Dr. W. Harris, president and chief executive officer, Science Foundation Arizona, Dr. Arthur Schneider and Dr. John P. Waszczak, director of advanced technologies, Raytheon, who skillfully and patiently supported and guided the joint effort to become a most promising technology program. The author also extends his thanks to the following consultants, suppliers, vendors of services, and so forth, who technically contributed to the project way beyond the call of duty:

JLA Technologies

Rock West solutions, Inc.

Curamik Electronics, Inc.

NxGEN Electronics, Inc.

Remtec, Inc.

EMCORE Corporation

PREFACE

The California Energy Commission Energy Research and Development Division supports public interest energy research and development that will help improve the quality of life in California by bringing environmentally safe, affordable, and reliable energy services and products to the marketplace.

The Energy Research and Development Division conducts public interest research, development, and demonstration (RD&D) projects to benefit California.

The Energy Research and Development Division strives to conduct the most promising public interest energy research by partnering with RD&D entities, including individuals, businesses, utilities, and public or private research institutions.

Energy Research and Development Division funding efforts are focused on the following RD&D program areas:

- Buildings End-Use Energy Efficiency
- Energy Innovations Small Grants
- Energy-Related Environmental Research
- Energy Systems Integration
- Environmentally Preferred Advanced Generation
- Industrial/Agricultural/Water End-Use Energy Efficiency
- Renewable Energy Technologies
- Transportation

Production of an Operating Photovoltaic Submodule for Integration into a High-Efficiency Conversion *Unit* is the final report for Contract Number 500-09-011 conducted by United Innovations, Inc. The information from this project contributes to Energy Research and Development Division's Energy Systems Integration Program.

For more information about the Energy Research and Development Division, please visit the Energy Commission's website at www.energy.ca.gov/research/ or contact the Energy Commission at 916-327-1551.

ABSTRACT

The goal of this project was to design, develop, and manufacture a high concentration photovoltaic power conversion unit that uses a photovoltaic cavity converter and advanced concentration triple junction solar cells to achieve higher solar to electric conversion rates than were previously possible. Photovoltaic cavity converters efficiently process the highly concentrated solar radiation into electricity. This system has the ability to recycle photons that are reflected from the surface of the cells in contrast with conventional flat, two-dimensional receivers where photon recycling is not possible and the reflected photons are lost to the conversion process. Triple junction solar cells are multi-junction cells that add junctions using different materials to capture more wavelengths of light, compared to single-junction cells that are tuned to only one wavelength of light.

Tests conducted under operational conditions outdoors demonstrated that the photovoltaic power conversion unit could achieve a system conversion efficiency improvement of 3 to 6 percent absolute and 12 to 24 percent relative when compared to a conventional flat photovoltaic receiver operating at 25 percent system efficiency. At about 200 suns concentration, researchers measured up to 53 percent relative improvement in system efficiency when compared to the system's performance with and without the front panel that enables the photon recycling.

Keywords: California Energy Commission, National Renewable Energy Laboratories, photovoltaic cavity converter, multijunction cells, photon recycling, parabolic dish and tracking system

Please use the following citation for this report.

Ortabasi, Ugur (United Innovations, Inc). 2010. *Production of an Operating Photovoltaic Submodule for Integration Into a High-Efficiency Conversion Unit*. California Energy Commission. CEC-500-2013-096.

TABLE OF CONTENTS

| Ackno | wledgementsi |
|--------|---|
| PREFA | ii |
| ABSTI | RACTiii |
| TABLE | E OF CONTENTSiv |
| LIST C | OF FIGURESv |
| LIST C | OF TABLESvii |
| EXECU | JTIVE SUMMARY1 |
| Int | troduction1 |
| Pr | oject Purpose1 |
| Pr | oject Results2 |
| Pr | oject Benefits2 |
| CHAP' | TER 1: Purpose |
| 1.1 | Introduction |
| 1.2 | Cell Series Resistance and Cell Performance |
| 1.3 | Photon Recycling in a Photovoltaic Cavity Converter |
| 1.4 | Objective of the Demonstration Project |
| 1.5 | Analytical Predictions of Cell Performance in a Cavity |
| CHAP' | TER 2: Technical Tasks14 |
| 2.1 | Task 2: Development of Resistivity Optimized Cells |
| 2.1 | .1 United Innovations Tasks |
| 2.1 | Deliverables 14 |
| 2.1 | .3 Memorandum on R-O Cells |
| 2.2 | Task 3: Procurement of Resistivity Optimized Cells |
| 2.2 | 2.1 UI Task Objective |
| 2.2 | 2.2 Deliverables |
| 2.2 | 2.3 Procured Cells |
| 2.3 | Task 4: Characterization of the Resistivity Optimized Cells by the Manufacturer19 |

| 2.4 | 20 | k 5: Verification R-O Cell Performance by National Renewable Energy Labo | ratories | | | |
|-------------|---------|---|------------|--|--|--|
| 2.4 | 1.1 | United Innovations Task Objectives | 21 | | | |
| 2.4 | 1.2 | Deliverables | 21 | | | |
| 2.5 Junc | | x 6: Design & Manufacture of an 8 x 8 Cell Photovoltaic Submodule of Triplessistivity-Optimized Cells | | | | |
| 2.5 | 5.1 | United Innovations Task Objectives | 21 | | | |
| 2.5 | 5.2 | United Innovations Task Objectives | 22 | | | |
| 2.5 | 5.3 | Deliverables | 22 | | | |
| 2.5 | 5.4 | Publicly Available Memorandum | 22 | | | |
| 2.5 | 5.5 | Production of the Functioning PV Submodule | 2 3 | | | |
| 2.5 | 5.6 | Satisfying the Performance Metrics: Photon Recycling and Conversion Effication 26 | ciency | | | |
| CHAP' | TER 3: | Photovoltaic Cavity Converter | 31 | | | |
| 3.1 | Opt | ical Design | 31 | | | |
| 3.2 | Stru | ctural Design | 32 | | | |
| 3.3 | Hea | t Exchanger Design | 32 | | | |
| 3.4 | | | | | | |
| CHAP' | TER 4: | Out-Door Test Facility | 37 | | | |
| 4.1 | Para | abolic Dish | 37 | | | |
| 4.2 | Trac | cking System | 38 | | | |
| 4.3 | PVC | CC/Dish Assembly and Operation | 39 | | | |
| CHAP' | TER 5: | Summary of Project Stage and Recommendations | 41 | | | |
| 5.1 | Reco | ommendations | 42 | | | |
| Glossa | ry | | 4 4 | | | |
| | | LIST OF FIGURES | | | | |
| Figure | 1: Hist | torical Improvement of Cell Efficiencies | 4 | | | |
| Figure | 2: Pow | ver Losses as a Function of Cell Series Resistance and Shading Losses | 5 | | | |
| Figure | 3: Prin | nciples of Photon Recycling | 6 | | | |

| Figure 4: Basic Optical Model and the Ideal Cavity Dimensions for Flux Uniformity | 7 |
|---|------|
| Figure 5: Solar Flux Uniformity in the Plane of the Solar Cells | 8 |
| Figure 6: CAD Drawing of the DBC Circuitry | 9 |
| Figure 7: Electro-Formed Mirror Masks Coated With Protected Silver (P = 98%) | 10 |
| Figure 8: Comparative Cell Optical Efficiency (COE) Study of Planar and Triangular Masks Various Center-to-Center Cell Distances | |
| Figure 9: Results of Optimization Study With a Single 37.1% Net Cell Efficiency | 13 |
| Figure 10: PVCC Performance Improvement Versus a "Single Hit" Design for Various COE's | s.13 |
| Figure 11: Off-the-Shelf EMCORE CTJ Cells Used as Baseline for This Project | 15 |
| Figure 12: Resistivity Optimized Cells as Delivered in Wafers | 18 |
| Figure 13: Photo Comparing the Contact Finger Grid Pitch of O-S and O-R Cells | 18 |
| Figure 14: A Sample of Test Records Provided by EMCORE | 19 |
| Figure 15: A Selected (Typical) IV-Plot for a Lot of About 40 Cells | 20 |
| Figure 16: Fully Integrated 8 X 8 Cell Solar Submodule | 23 |
| Figure 17: Circuitry Pattern and Critical Dimensions for the 8 X 8 Cell Photovoltaic Submodu on a 5" X 5" DBC Substrate | |
| Figure 18: Rendering of the Etched Solar Sub-Array Layout on DBC Substrate | 24 |
| Figure 19: Address Codes for the Cells and the Strings on the Actual Solar PV Submodule Subarray | 25 |
| Figure 20: One Sun Testing Photovoltaic Submodule to Validate the Functioning of the Unit | 25 |
| Figure 21: Cross-Sectional Schematic of the Water-Cooled Photovoltaic Submodule | 27 |
| Figure 22: String I-V Plot Obtained With a SPIRE 800 Array Tester With Three Wire Meshes Place (69.4W/String Available Solar Power) | |
| Figure 23: Exploded View of PVCC Showing the Mirrorized Front and Side Panels | 31 |
| Figure 24: CAD Oblique Cross-Cut of the Fully Assembled PVCC | 32 |
| Figure 25: CAD Drawing of the Forced Water Heat Exchanger | 33 |
| Figure 26: Machined Top and Bottom Parts of the Heat Exchanger Prior to Brazing | 33 |
| Figure 27: Photo of PVCC "Rear End" Assembly | 34 |
| Figure 28: "Rear Assembly" as Integrated Into the PVCC Housing | 34 |
| Figure 29: Junction Box Containing the Bypass Diode Board Is Being Attached to the Heat Exchanger | 35 |
| Figure 30: Photo of PVCC Showing the Front Panel With the Cavity Aperture | 35 |

| Figure 31: PVCC :Back Plate- Attachment Platform to Interface With the Dish36 |
|--|
| Figure 32: Photo of Test Ready PVCC Prototype |
| Figure 33: All-Glass, Parabolic Dish Designed and Built by University of Arizona in Conjunction With This Project: Diameter = 2.5m, F-Number = 0.6, Back-Surface Mirror, Effective Reflectance = 88.5% |
| Figure 34: Support Structure and Sun-Tracking System Designed and Integrated by Raytheon in Conjunction With This Project |
| Figure 35: Outdoors Solar Test Facility Built and Operated by Tucson Embedded Systems 38 |
| Figure 36: PVCC Mounted on the Dish and Tracking the Sun |
| Figure 37: Photo Showing Installed PVCC Provided With Cooling and Power Lines40 |
| Figure 38: PVCC Tracking the Sun at 700 Suns Concentration (Thermal Test) |
| Figure 39: Project Technology Road Map for a Successful Market Entry by 201543 |
| |
| LIST OF TABLES |
| Table 1: HCPV Systems Using III-V Cells |
| Table 2: Optimized R-O Cell Design Parameters and Comparison to O-S-Cells Concentration Ratio Cr = 500 X SUNS |
| Table 3: Distribution of Conversion Efficiency of Delivered Cells |
| Table 4: Photon Recycling Data and Results |
| Table 5: Preliminary Conversion Efficiency Results |

EXECUTIVE SUMMARY

Introduction

Photovoltaic power is the conversion of energy from the sun into electricity. Multi-junction solar cells used in high concentration photovoltaic (HCPV) cells have enabled record-breaking efficiencies in electricity generation from the sun's energy and have the potential to make solar electricity cost-effective at the utility scale. System efficiencies for single cell HCPV receivers remain below 25 percent, however. The decrease in system conversion efficiency is caused by many loss mechanisms involved in the sun light-to-electricity conversion process. One overriding loss mechanism at high concentrations (500 suns and above) is the back reflection of light from the surface of the receiving cells, causing a reduction in the amount of concentrated light that is available for the conversion process. There are two causes of the back reflection: 1) the residual reflectance of the active cell area; and 2) the reflectance from the cell contact grid. Another loss mechanism that occurs in multi cell receivers is caused by the non-active cell areas around the cells that may reflect and/or absorb the incident focused light. The most effective way to reduce the reflective losses is by making the contact fingers very thin and using a minimum amount of them per unit area to conduct the photo-current. However, such a reduction in the contact grid leads to cell series resistance losses that limit how thin one can make the contact grid fingers and how few of them can be used per unit area. High efficiency, reduced manufacturing cost, and availability of abundant direct sunlight are the key components necessary for high-concentration photovoltaic systems to compete with fossil fuel generated electricity.

Project Purpose

The goal of this project was to design, develop, and manufacture a high concentration photovoltaic power conversion unit that uses a photovoltaic cavity converter (PVCC) and advanced concentration triple junction solar cells to reach solar-to-electric conversion efficiencies in excess of 40 percent. Photovoltaic cavity converters efficiently process the highly concentrated solar radiation into electricity. This system has the ability to recycle photons that are reflected from the surface of the cells in contrast with conventional flat, two-dimensional receivers where photon recycling is not possible and the reflected photons are lost to the conversion process. Triple junction solar cells are multi-junction cells that add junctions using different materials to capture more wavelengths of light, compared to single-junction cells that are tuned to only one wavelength of light. This concept could become the most efficient high-concentration photovoltaic system developed to date if the goal of 40 percent solar-to-electric conversion efficiency can be met. The comparable cost of electricity targeted for the overall project was 5 to 7 cents per kilowatt hour (kWh) for utility applications in the southwestern United States.

The specific objectives of the project were to use off-the-shelf and resistivity optimized cells to experimentally verify:

1. The inherent photon recycling advantage of PVCC systems over conventional systems.

2. The relative performance of the resistivity-optimized (R-O) cell design compared to the off-the-shelf (O-S) cell design. Resistivity refers to the internal resistance of the material used to make the solar cells.

Project Results

The key advantage of the design was the use of a PVCC as the receiver. PVCCs efficiently process highly concentrated solar radiation into electricity by recycling photons that are reflected from the surface of the cells. Conventional flat, two-dimensional receivers cannot recycle photons and the reflected photons are lost to the conversion process.

This project was funded by the California Energy Commission and is the second phase of a two-part demonstration program. Raytheon/University of Arizona and the Science Foundation Arizona funded the first phase of this program. Both phases were designed to demonstrate the performance improvement that is achievable by using a PVCC receiver with high photon recycling efficiency. Although both phases used the same PVCC/dish configuration, the grid contact design of the respective cells was different. Phase 1 used conventional, off-the-shelf, high-concentration triple-junction cells made by EMCORE. Triple junction solar cells are multijunction cells that add junctions using different materials to capture more wavelengths of light, compared to single-junction cells that are tuned to only one wavelength of light. Phase 2 used the same concentration triple-junction cells with a contact grid finger design for enhanced performance in a cavity environment.

The research team conducted tests under operational conditions outdoors. The test results indicated that the targeted 3 to 6 percent increase in system efficiency over conventional high concentration photovoltaic systems was achievable. At about 200 suns concentration, researchers measured up to 53 percent relative improvement in system efficiency when compared to the system's performance with and without the front panel that enables the photon recycling.

The authors recommended that development and demonstration of the PVCC system be continued in order to reach a pilot plant stage and ultimately, a fully commercialized product.

Project Benefits

High concentration photovoltaic technology advances will help make solar power competitive with less expensive ways of generating electricity, such as coal- oil- or gas-fired power plants. The increased use of solar power will reduce greenhouse gas emissions that cause climate change as well as reduce other emissions that cause air pollution and the resulting detrimental health effects.

CHAPTER 1: Purpose

1.1 Introduction

Multi-junction solar cells used in High Concentration Photovoltaics (HCPV) have enabled record-breaking efficiencies in electricity generation from the Sun's energy, and have the potential to make solar electricity cost-effective at the utility scale. Figure 1 shows the historical improvement in cell conversion efficiencies over the last three decades until year 2008. This year (2010) the performance of the advanced triple junction cells reached 41.7 percent, a world record established by Fraunhofer Institute in Germany. Despite these excellent cell performances the respective system efficiencies for single cell HCPV receivers remain systematically below 25 percent (Table 1). The decrease in system conversion efficiency is caused by many loss mechanisms involved in the sun light-to-electricity conversion process. One overriding loss mechanism at high concentrations (500 suns and above) is the back reflection of light from the surface of the receiving cells, and therefore a reduction in the amount of concentrated light that is available for the conversion process. The cause of the back reflection is twofold: a) The residual reflectance (after AR coating) of the active cell area and b) the reflectance from the cell metallization (cell contact grid). Another loss mechanism that occurs in multi cell receivers (for example, dense arrays) is caused by the non-active cell areas around the cells that may reflect and/ or absorb the incident focused light. It is desirable to reduce the reflective losses by making the contact fingers very thin and use a minimum amount of them per unit area to conduct the photo-current. However, such a reduction in the top metallization area (contact grid) leads to the well known problem of cell series resistance losses that limit how thin one can make the contact grid fingers and how few of them can be used per unit area.

Figure 1: Historical Improvement of Cell Efficiencies

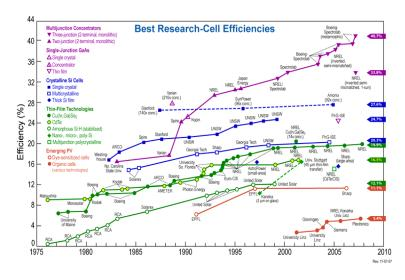


Table 1: HCPV Systems Using III-V Cells

Table 1. HCPV systems using R-V cells. n_ module efficiency, n_: system efficiency. Some of the presented efficiencies here are given by the system developer but are still unweithed.

| Company | | Optics | X | Cell/receiver | | $\eta_{\rm m}$ (%) | η_s (%] |
|------------------------|-----------|--------------------------------|------|---------------|-------------------------|--------------------|--------------|
| Arima Eco Energy | Taiwan | Fresnel lens | 476 | Spectrolab | 1 cm ² | 22-25 | - |
| Concentrix Solar | Germany | Fresnel lens | 385 | Azur | d = 2.3 mm | 27 | 23.5 |
| DaidoSteel | Japan | Fresnel lens | 550 | Azur | 49 mm ² | 23 | 21 |
| Delta Electronics | Taiwan | Fresnel lens | 470 | Spectrolab | 1 cm ² | 26 | 23 |
| Emcore | USA | Fresnel lens | 500 | Emcore | 1 cm ² | _ | 27 |
| Energy Innovations | USA | Fresnel lens | 1440 | Emcore | 1 cm ² | 28.8 | 23-25 |
| Enfocus Engineering | USA | Fresnel lens | >300 | - | 1 cm ² | >20 | - |
| Green and Gold | Australia | Fresnel lens | 1370 | Emcore | 1 cm ² | 34 | 28 |
| INER | Taiwan | Fresnel lens | 476 | Spectrolab | 1 cm ² | 23 | 20 |
| Opel International | USA | Fresnel lens | 500 | Spectrolab | 1 cm ² | 26-28 | - |
| PyronSolar | USA | Fresnel lens | 500 | Spectrolab | 1 cm ² | 22 | 21 |
| Sharp | Japan | Fresnel lens | 700 | Sharp | 49 mm ² | - | - |
| SolarTec | Germany | Fresnel lens | 600 | ENE | 4 mm ² | 20 | 17 |
| Sol3G | Spain | Fresnel lens | 476 | Azur | 30 mm ² | 24 | 22.7 |
| Sunrgi | USA | Fresnel lens | 2000 | Spectrolab | 1 cm ² | - | - |
| Isofoton | Spain | Totalinternal reflection lens | 1000 | - | 1 mm ² | 25 | 23 |
| GreenVolts | USA | Micro-Dish | 625 | Spectrolab | 1 cm ² | 28.5 | _ |
| Solfocus | USA | Micro-Dish | 500 | Spectrolab | 1 cm ² | 25 | 23 |
| | | Dish & dense | | | | | |
| Solar Systems | Australia | array receiver | 500 | Spectrolab | 1536×1 cm ² | 35 | 30 |
| Cool Earth Solar | USA | Dish & dense array receiver | 400 | - | - | 30 | - |
| Menova Energy | Canada | Segmented reflector | 1450 | Émcore | $116\times1\text{cm}^2$ | 26.4 | 23.2 |

1.2 Cell Series Resistance and Cell Performance

These cell series resistance losses become the major limiting mechanism to the overall cell performance at higher concentrations. As the photo current grows linearly with the increasing concentration, the associated resistive heating losses grow according to Joule's first law I²xR. Thus an increasing part of the photo-current is dissipated as heat. As a result the design of conventional (one hit) high concentration cells requires a "compromise" solution that keeps the reflective losses and the resistive losses in balance to be able to achieve the optimum possible high efficiency.

Figure 2 below represents the optimization calculations for the following assumptions:

- A 10 mm x 10 mm, 3J concentrator cell with a conversion efficiency = 31 percent @ 500 suns
- Parallel Grid Finger Spacing is to be determined (TBD) as a result of optimization
- Grid Finger width is 10 μm
- MetalFingers cover ~ 10 percent of the active area

Result: The minimum relative loss of ~ 15 percent is achieved at ~ 100 μ m grid finger spacing and 10 μ m grid finger width

Conclusion: A near ideal Photovoltaic Cavity Converter that mitigates the series resistance losses and effective shading (obstruction) losses can increase the net efficiency gains of the same 31 percent cell by about 15 percent (relative) or ~4.7 percent absolute.

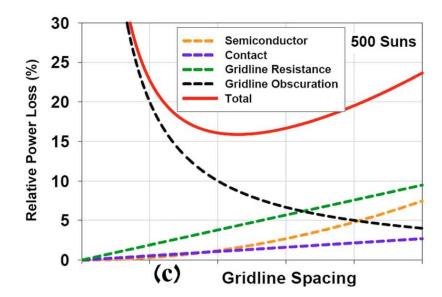


Figure 2: Power Losses as a Function of Cell Series Resistance and Shading Losses

1.3 Photon Recycling in a Photovoltaic Cavity Converter

Photon recycling process in a cavity is shown in Figure 3. This concept of photon re-utilization after the "first hit" can help to mitigate the cell series resistance- and effective shading losses if, designed very carefully. It is worthwhile to mention that the reflective loses and the escape of photons from the cavity may "wash-off" the benefits if these are not minimized to a great extent. Also the Kaleidoscopic cavity dimensions must be chosen such that the resulting flux density distribution in the plane of the Photovoltaic Sub-Module must be uniform within 2 percent RMS.

Slide No. 2

RECYCLED PHOTON

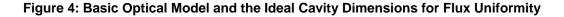
Is Photon Absorbed By The Active Area Of The Cell?

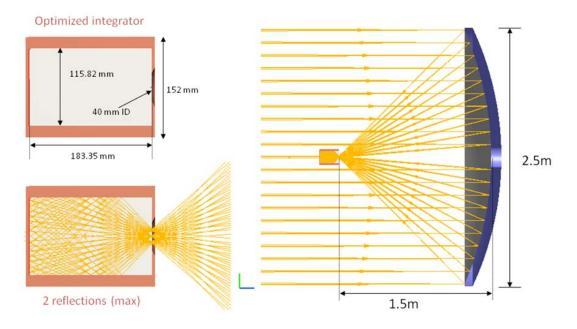
Available to Generate Photocurrent

Figure 3: Principles of Photon Recycling

PRINCIPLES OF PHOTON RECYCLING

Figure 4 shows the basic optical model we developed and the calculated cavity dimensions that provide the flux distribution uniformity that is required.





Excellent flux uniformity obtained in the plane of the Photovoltaic Sub-Module is shown in Figure 5. The "X" shaped reddish pattern stems from the shadowing struts that are used to support the photovoltaic cavity converter (PVCC). However, these are within the limits of 2 percent RMS. Figure 5 also shows the location of the reflective mask (98 percent reflective) which covers the non-active areas between the cells and returns the photons hitting these areas back into the re-cycling process (Figure 6). In this project two different mask geometries were considered: a) Flat, 2-D and b) Triangular, 3D. Figure 6 shows the results of our optical studies for predicting the "Optical Cavity Efficiency" (OCE). OCE is defined as the probability of a photon to be counted (enters a cell) after it is reflected following the first hit. For the scope of this study we chose flat, 2D mask as it was lower risk to fabricate those.

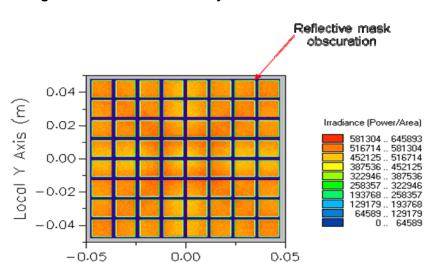


Figure 5: Solar Flux Uniformity in the Plane of the Solar Cells

The particular solar array design for this project requires a center-to-center cell distance of 13.07 mm (see Figure 6). However, the mirrored mask is designed slightly larger (13.2 mm) to cover the thin regions of dead areas around the cells. This represents a very large (38 percent) non-active area ("streets") between the cells that would deteriorate the performance of the PVCC module dramatically if no mirror mask is used.

Local X Axis (m)

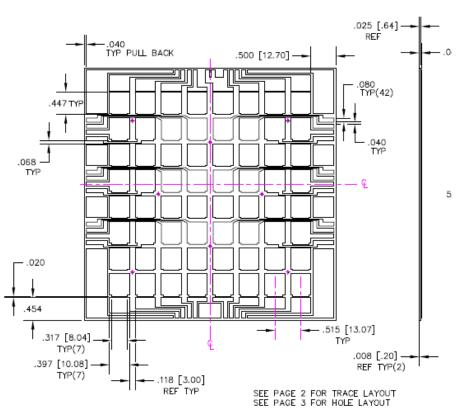


Figure 6: CAD Drawing of the DBC Circuitry

Thus to avoid these losses in the actual design the streets are covered with a planar mirror mask of high reflectivity (98 percent) shown in Figure 7. This recovers most of the photons that would strike otherwise the non-active area and would be lost to the conversion process. As we found during the experimental testing the respective improvement could be as high as 53 percent for this particular design (see experimental results).

Figure 7: Electro-Formed Mirror Masks Coated With Protected Silver (P = 98%)

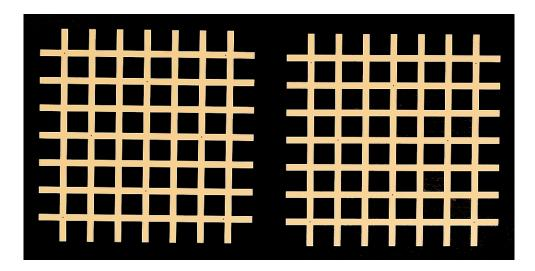


Figure 8 shows the results of our ray-tracing studies to determine the Cavity Optical Efficiency (COE) for both: Flat, 2D and Triangular, 3D mirror masks as a function of center-to-center cell distance. This distance was determined by the practical design requirements for the DBC substrate to allow by-pass diode lines to be incorporated. For the sake of this study designers chose the distance to be 13.2 mm, leaving a gap of about 2.4 mm between the cells. This leads to a surprisingly high dead area of about 38 percent underneath the Flat, 2D mirror mask across the array. However, in the cavity design 81 percent of the reflections from the mask will be ultimately counted by the cells. This reduces the effective dead area to only 7.2 percent across the array.

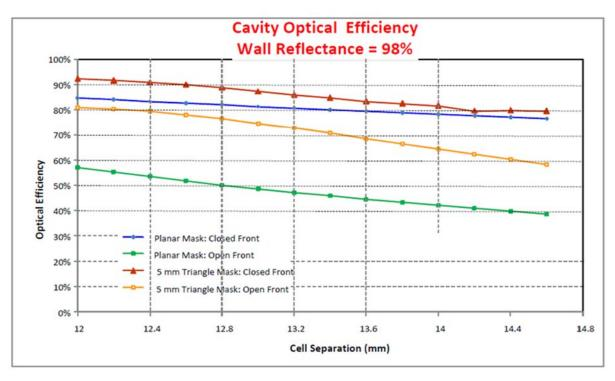


Figure 8: Comparative Cell Optical Efficiency (COE) Study of Planar and Triangular Masks at Various Center-to-Center Cell Distances

<u>Note:</u> COE is defined as the probability of a reflected photon to enter a cell and become available to generate photo-current.

1.4 Objective of the Demonstration Project

The key advantage of our approach comes from the use of a Photovoltaic Cavity Converter (PVCC) as the receiver that converts the highly concentrated solar radiation into electricity. PVCC has the unique capability of re-cycling photons that are reflected from the surface of the cells after the "first hit". In the case of conventional "flat" receivers the photon recycling is not possible and the reflected photons are reflected back into the surrounding without the possibility of recycling them to boost the performance.

The present project funded by the California Energy Commission is the second phase of a two-phase demonstration program. Phase 1 was funded by Raytheon/University of Arizona and the Science Foundation Arizona. Both phases are designed to demonstrate the performance improvement that is achievable using a PVCC receiver that re-cycles photons. Although both phases use the same PVCC/Dish configuration, the grid contact design on the cells is different. Phase 1 uses off-the-shelf high concentration triple-junction cells (CTJ made by EMCORE for "One Hit" systems) whereas, Phase 2 uses same CTJ cells that have a modified contact grid design for optimal performance in a cavity environment.

The purpose of these demonstration projects with off-the-shelf and resistivity optimized cells was to experimentally verify:

- 3. The inherent photon re-cycling advantage of PVCC systems over the conventional "One Hit" systems, as well as
- 4. The relative performance of the Resistivity- Optimized (R-O) cell design as compared to the Off-the-Shelf (O-S) cell design.

To assess the potential of performance improvement of the photon recycling efficiency we developed an analytical model that involves the operation of the cell in a cavity environment. The model has the option to remove the cavity effect for the purposes of comparison. The model requires prior knowledge of the Cavity Optical Efficiency (COE) as a known input parameter. For the results shown below the COE was selected to be 81 percent, see Figure 8.

1.5 Analytical Predictions of Cell Performance in a Cavity

The analytical model to predict the performance of cell within a cavity assumes only one single cell unit completely covering the sub-array plane at the back-wall of the cavity. This assumption underestimates the performance of a cell array that consists of multiple cells which populate the back-wall of the cavity. In our present design we have a matrix of 8×8 cells.

Figure 9 summarizes the analytical modeling studies for a single cell with 37.1 percent net efficiency.

The model obtains the best efficiency for a given COE by minimizing the cell series resistance (adding more grid fingers, such as, reducing finger pitch) and reducing the effective shading losses. The plots in Figure 9 show that at a concentration of 500 suns the cavity with 81 percent COE improves the performance by 2.6 percent absolute or 6.5 percent relative. Figure 10 shows how the overall conversion efficiency increases as the Cavity Optical Efficiency (COE) improves. At a practically achievable COE of 90 percent the cell-cavity efficiency becomes 40 percent corresponding to an efficiency gain of 2.9 percent absolute and 7.8 percent relative.

Figure 9: Results of Optimization Study With a Single 37.1% Net Cell Efficiency

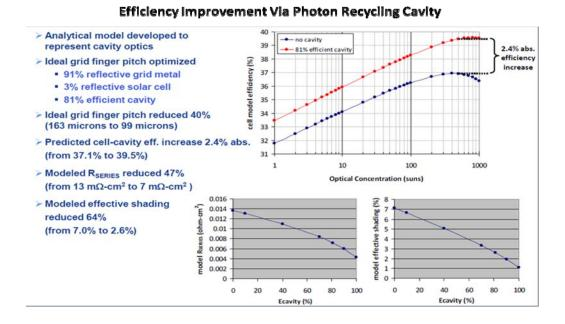
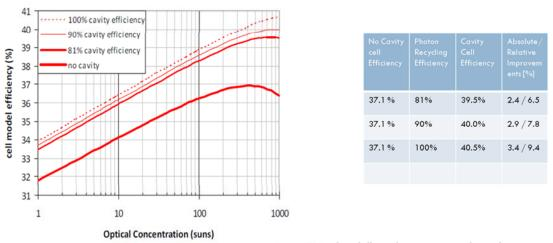


Figure 10: PVCC Performance Improvement Versus a "Single Hit" Design for Various COE's



PVCC Performance Improvement Against a "Single Hit" Design as a Function of Photon Recycling Efficiency

CHAPTER 2: Technical Tasks

2.1 Task 2: Development of Resistivity Optimized Cells

Conventional off-the-shelf (O-S) EMCORE concentrator cells are designed to work optimally with Fresnel optics and flat, 2D PV receivers. They are not optimal for the cavity receivers such as PVCC. In this task, United Innovations will develop, in conjunction with technical consultants (EMCORE), special resistivity optimized (R-O) 3j cells that benefit from photon recycling capability of the PVCC.

2.1.1 United Innovations Tasks

- Identify design parameters for R-O cells
- Communicate design parameters to EMCORE technical partners
- Manage the development and manufacture of R-O cells that will benefit from photon recycling

2.1.2 Deliverables

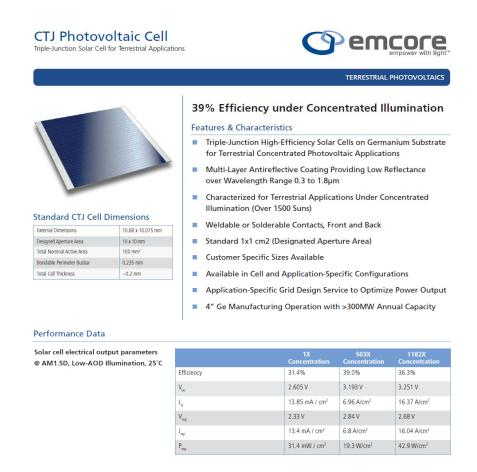
Memorandum on R-O cells that includes a discussion that fully addresses each of the following questions:

- What were the design parameters that were used?
- Were the design parameters used successfully implemented?
- Were there any problems issues during manufacturing?
- What was the cost of manufacturing? Was it less or more costly than expected?
- How long was the manufacturing process? Was it short or longer than expected?
- Overall, was the manufacturing process successful?

2.1.3 Memorandum on R-O Cells

For the purposes of this study the physical cell dimensions of the R-O cells were chosen to be the same as S-O cells such as, $10.68~mm \times 10.075~mm \times 180~\mu m$. The specifications of the CTJ O-S cells are shown on Figure 11.

Figure 11: Off-the-Shelf EMCORE CTJ Cells Used as Baseline for This Project



The nominal efficiency of these CTJ cells is 39 percent. However, the S-O cells we purchased had a skewed bell shaped distribution ranging from 35 to 38 percent.

To identify the design parameters and predict their impact on the cell performance, we developed a cell analytical model for a cavity environment. The analytical results are discussed under in the Analytical Predictions of Cell Performance in a Cavity section. The predictions are summarized in Table 2 below.

Table 2: Optimized R-O Cell Design Parameters and Comparison to O-S-Cells Concentration Ratio Cr = 500 X SUNS

| Fixed Key Cell and Cavity Parameters | Value | Optimized Key Cell Parameter | From | То | Change from O-S Cell |
|--|-------|--------------------------------------|-----------|----------|---|
| Reflectance of Grid Metal | 91% | Grid Finger Pitch | 163 µm | 99 µm | 40% drop |
| Reflectance of AR Coated Cell | 3% | Cell Series Resistance | 13 mΩ-cm² | 7 mΩ-cm² | 47% drop |
| Cavity Photon Recycling Efficiency | 81% | Effective Shading | 7% | 2.6% | 64% drop |
| | | Single Cell-in- Cavity Efficiency | 37.1% | 39.5% | 2.4% rise (abs.) 6.5% rise (rel.) |
| Cavity Photon Recycling Efficiency | 90% | Single Cell-in- Cavity Efficiency | 37.1% | 40.0% | 2.9% rise (abs.) 7.8% rise (rel.) |
| Cavity Photon Recycling Efficiency | 95% | Single Cell-in- Cavity Efficiency | 37.1% | 40.5% | 3.4% rise (abs.) 9.2% rise (rel.) |

Note: As mentioned before the above analytical results are for a single cell in a cavity that covers the total target area. In the case of multi-cell receivers (e.g. dense arrays), the relative gain that is achievable with the use of a Mirror Mask can be much higher.

There were no technical problems or issues during manufacturing. The total cost for the 210 cells, including the non-reoccurring engineering costs and optimization studies, was \$52,753. Excluding the NRE cost and the cost of analytical optimization studies, EMCORE charged 15,000 for 210 cells or \$1930.5/W. At a concentration of 500 X suns and 37 percent conversion efficiency this translates into \$3.86/W. This is about 7 to 8 times more than the targeted cost of about \$0.5/W for cell that is required for the photovoltaic (PV) to become competitive.

The manufacturing process, or more accurately the lead time to delivery, was much longer than expected (12 -16 weeks instead 3-4 weeks). Overall, the manufacturing process was very successful.

2.2 Task 3: Procurement of Resistivity Optimized Cells

The original goal of this task was to procure 165 units of advanced R-O 3j cells from EMCORE having the physical dimensions: 1,258 x 1.258 and are optimized for 500 suns. A set of 165 cells will provide two complete 64 (eight by eight) cell sets plus 20 percent spare cells for possible

repairs. With the concurrence of the Energy Commission Contract Manager, the dimensions and the number of the cells has been changed to 10.68 mm x 10.075 mm and 210, respectively. A set of 210 cells will provide three complete 64 (eight x eight) cell sets plus 8 percent spare cells for future repairs. The change in cell dimensions was done to be able to use EMCORE's standard O-S cells thus avoiding the exorbitant cost of a "new line" of cells. The number of cells was increased to be able to have a third complete Photovoltaic Sub-Module. In our previous project with O-S cells (UI/Raytheon project), we experienced several thermal damages at high concentrations and lost two sub-arrays. A third spare sub-array minimizes the risk.

2.2.1 UI Task Objective

- Procurement verification of the triple junction R-O cell
- CPR

2.2.2 Deliverables

- A set of 210 cells with physical dimensions: 10.68 x 10.075 mm optimized for 500x suns
- CPR

2.2.3 Procured Cells

EMCORE delivered 210 Resistivity –Optimized cells in 10 separate wafers. The photo in Figure 12 shows the cells before they were removed from the wafers they were shipped in. Some of the cells had obscurities on the surface, but the test data at 500 suns did not indicate any degradation in their performance.



Figure 12: Resistivity Optimized Cells as Delivered in Wafers

Figure 13 shows the modification made to the Contact Finger Grid Pitch.

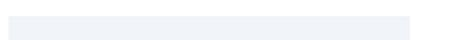
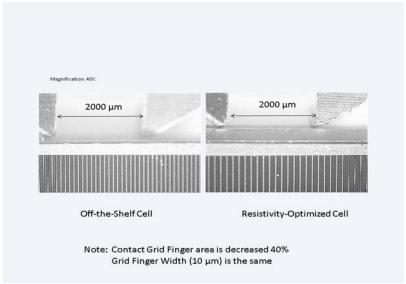


Figure 13: Photo Comparing the Contact Finger Grid Pitch of O-S and O-R Cells



2.3 Task 4: Characterization of the Resistivity Optimized Cells by the Manufacturer

Characterization of the R-O cells was performed by EMCORE in their Plant. Each cell manufactured was tested for Open Circuit Voltage (Voc in Volts), Short Circuit Current (Isc in A/cm²), Fill Factor (FF in percent), Responsivity (in A/W) and Efficiency (η , in percent). All tests were done around 500 suns, however for each test the exact value of the flux density was determined anew. Figure 14 shows the standard recording format as used by EMCORE.

Figure 14: A Sample of Test Records Provided by EMCORE

| Di | e Location | 1 | CXN _{DUT} | Voc | J _{SC} | I _{SC} | FF | Efficiency | responsivity | area | Irrad _{1-SUN} |
|-----------|------------|---------------------------|--------------------|---------|-----------------|-----------------|------|------------|--------------|--------------------|------------------------|
| Total Die | on Tray | cell ID | (Suns) | (Volts) | (A/cm2) | (Amps) | (%) | (%) | (A/W) | (cm ²) | (W/m ²) |
| 1 | 1 | 133271_3_3_1_080510105530 | 520.1 | 3.161 | 7.19 | 7.19 | 86.6 | 37.83 | 0.1382 | 1.000 | 1000 |
| 2 | 2 | 133271_3_4_1_080510105529 | 531.7 | 3.166 | 7.24 | 7.24 | 87.0 | 37.50 | 0.1361 | 1.000 | 1000 |
| 3 | 3 | 133271_3_5_1_080510105529 | 506.7 | 3.164 | 7.01 | 7.01 | 86.4 | 37.79 | 0.1383 | 1.000 | 1000 |
| 4 | 4 | 133271_3_6_1_080510105528 | 500.6 | 3.163 | 6.82 | 6.82 | 86.9 | 37.40 | 0.1362 | 1.000 | 1000 |
| 5 | 6 | 133271_3_2_2_080510105523 | 506.0 | 3.160 | 7.03 | 7.03 | 86.3 | 37.87 | 0.1389 | 1.000 | 1000 |
| 6 | 7 | 133271_3_3_2_080510105523 | 505.3 | 3.165 | 6.95 | 6.95 | 86.7 | 37.75 | 0.1376 | 1.000 | 1000 |
| 7 | 8 | 133271_3_4_2_080510105524 | 523.8 | 3.170 | 7.20 | 7.20 | 86.9 | 37.88 | 0.1375 | 1.000 | 1000 |
| 8 | 9 | 133271_3_5_2_080510105525 | 540.0 | 3.172 | 7.33 | 7.33 | 87.2 | 37.57 | 0.1358 | 1.000 | 1000 |
| 9 | 10 | 133271_3_6_2_080510105525 | 519.5 | 3.171 | 7.15 | 7.15 | 87.0 | 37.99 | 0.1377 | 1.000 | 1000 |
| 10 | 11 | 133271_3_7_2_080510105526 | 512.8 | 3.169 | 6.95 | 6.95 | 87.5 | 37.55 | 0.1355 | 1.000 | 1000 |
| 11 | 12 | 133271_3_8_2_080510105527 | 518.2 | 3.165 | 7.03 | 7.03 | 87.8 | 37.71 | 0.1357 | 1.000 | 1000 |
| 12 | 13 | 133271_3_2_3_080510105522 | 503.1 | 3.162 | 6.95 | 6.95 | 87.1 | 38.02 | 0.1381 | 1.000 | 1000 |
| 13 | 14 | 133271_3_3_3_080510105521 | 523.7 | 3.168 | 7.17 | 7.17 | 87.0 | 37.72 | 0.1369 | 1.000 | 1000 |
| 14 | 15 | 133271_3_4_3_080510105521 | 522.8 | 3.170 | 7.16 | 7.16 | 87.1 | 37.85 | 0.1371 | 1.000 | 1000 |
| 15 | 16 | 133271_3_5_3_080510105520 | 515.5 | 3.169 | 6.98 | 6.98 | 87.5 | 37.57 | 0.1354 | 1.000 | 1000 |
| 16 | 17 | 133271_3_6_3_080510105519 | 493.6 | 3.167 | 6.79 | 6.79 | 87.1 | 37.95 | 0.1376 | 1.000 | 1000 |
| 17 | 18 | 133271_3_7_3_080510105519 | 524.0 | 3.172 | 7.17 | 7.17 | 86.9 | 37.74 | 0.1369 | 1.000 | 1000 |
| 18 | 19 | 133271_3_8_3_080510105518 | 511.5 | 3.169 | 6.99 | 6.99 | 87.1 | 37.72 | 0.1367 | 1.000 | 1000 |
| 19 | 21 | 133271_3_2_4_080510105513 | 502.4 | 3.161 | 6.93 | 6.93 | 86.8 | 37.87 | 0.1380 | 1.000 | 1000 |
| 20 | 22 | 133271_3_3_4_080510105513 | 506.0 | 3.165 | 7.02 | 7.02 | 86.3 | 37.89 | 0.1387 | 1.000 | 1000 |
| 21 | 24 | 133271_3_5_4_080510105515 | 506.3 | 3.168 | 6.94 | 6.94 | 87.0 | 37.80 | 0.1372 | 1.000 | 1000 |
| 22 | 25 | 133271_3_6_4_080510105515 | 511.9 | 3.169 | 6.98 | 6.98 | 87.2 | 37.67 | 0.1364 | 1.000 | 1000 |
| 23 | 26 | 133271_3_7_4_080510105516 | 530.2 | 3.174 | 7.21 | 7.21 | 87.3 | 37.67 | 0.1360 | 1.000 | 1000 |
| 24 | 27 | 133271_3_8_4_080510105517 | 528.8 | 3.172 | 7.21 | 7.21 | 87.1 | 37.68 | 0.1364 | 1.000 | 1000 |
| 25 | 28 | 133271_3_9_4_080510105517 | 515.7 | 3.171 | 7.14 | 7.14 | 86.9 | 38.15 | 0.1385 | 1.000 | 1000 |
| 26 | 29 | 133271_3_1_5_080510105511 | 501.1 | 3.145 | 6.89 | 6.89 | 86.1 | 37.23 | 0.1375 | 1.000 | 1000 |
| 27 | 31 | 133271_3_3_5_080510105510 | 520.5 | 3.165 | 7.17 | 7.17 | 86.3 | 37.66 | 0.1378 | 1.000 | 1000 |
| 28 | 32 | 133271_3_4_5_080510105509 | 531.6 | 3.168 | 7.26 | 7.26 | 87.1 | 37.71 | 0.1366 | 1.000 | 1000 |
| 29 | 33 | 133271_3_5_5_080510105509 | 504.5 | 3.167 | 6.95 | 6.95 | 86.3 | 37.67 | 0.1378 | 1.000 | 1000 |
| 30 | 34 | 133271_3_6_5_080510105508 | 513.1 | 3.169 | 7.03 | 7.03 | 86.7 | 37.62 | 0.1369 | 1.000 | 1000 |
| 31 | 35 | 133271_3_7_5_080510105507 | 519.0 | 3.170 | 7.09 | 7.09 | 87.4 | 37.82 | 0.1366 | 1.000 | 1000 |
| 32 | 37 | 133271_3_9_5_080510105506 | 508.0 | 3.169 | 6.99 | 6.99 | 86.6 | 37.76 | 0.1376 | 1.000 | 1000 |
| 33 | 38 | 133271_3_2_6_080510105501 | 513.9 | 3.155 | 7.08 | 7.08 | 86.7 | 37.69 | 0.1378 | 1.000 | 1000 |
| 34 | 39 | 133271_3_3_6_080510105502 | 510.6 | 3.160 | 7.04 | 7.04 | 86.8 | 37.81 | 0.1379 | 1.000 | 1000 |
| 35 | 40 | 133271_3_4_6_080510105503 | 534.2 | 3.164 | 7.28 | 7.28 | 86.8 | 37.45 | 0.1364 | 1.000 | 1000 |
| 36 | 41 | 133271_3_5_6_080510105503 | 525.8 | 3.167 | 7.22 | 7.22 | 86.7 | 37.69 | 0.1373 | 1.000 | 1000 |
| 37 | 42 | 133271_3_6_6_080510105504 | 517.4 | 3.167 | 7.17 | 7.17 | 86.7 | 38.04 | 0.1385 | 1.000 | 1000 |
| 38 | 44 | 133271_3_8_6_080510105505 | 524.3 | 3.169 | 7.09 | 7.09 | 87.4 | 37.47 | 0.1353 | 1.000 | 1000 |
| 39 | 45 | 133271_3_3_7_080510105500 | 521.8 | 3.153 | 7.15 | 7.15 | 86.9 | 37.55 | 0.1370 | 1.000 | 1000 |
| 40 | 46 | 133271_3_4_7_080510105500 | 536.4 | 3.162 | 7.39 | 7.39 | 86.9 | 37.86 | 0.1378 | 1.000 | 1000 |
| 41 | 48 | 133271_3_6_7_080510105458 | 516.9 | 3.163 | 7.13 | 7.13 | 86.5 | 37.76 | 0.1379 | 1.000 | 1000 |
| 42 | 49 | 133271_3_7_7_080510105458 | 507.4 | 3.161 | 6.93 | 6.93 | 86.6 | 37.42 | 0.1366 | 1.000 | 1000 |
| 43 | 50 | 133271_3_4_8_080510105456 | 499.0 | 3.135 | 6.79 | 6.79 | 86.8 | 37.01 | 0.1360 | 1.000 | 1000 |

The recorded test data provided by EMCORE was accompanied by typical IV-Plot for every batch of about 40 cells. An example IV plot is given in Figure 14 for the cell with the ID No. $133271_3_4_3_080510105521$. For this specific cell (ID $133271_3_4_3_80510105521$) we read the determined performance parameters from Figure 15 as follows: Voc = 3.170 V, Isc = 7.16 mA, FF = 88 percent, $\eta = 37.85$ percent, Responsivity = 0.1371 A/W.

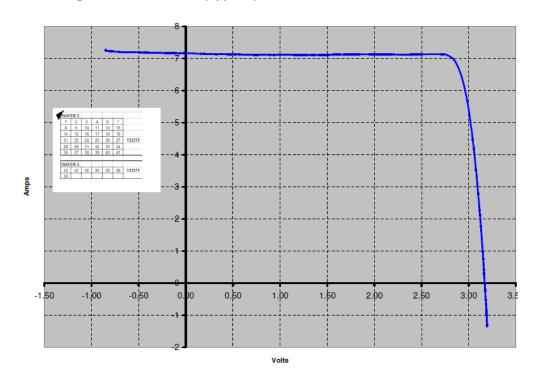


Figure 15: A Selected (Typical) IV-Plot for a Lot of About 40 Cells

The statistical variation of the measured efficiencies for these R-O cells is remarkably narrow, sharply peaking in the 37 percent bracket. Table 3 roughly shows the efficiency distribution of the delivered cells among the measured percentage brackets.

Conclusion: Delivered R-O cells meet the performance criteria (efficiency) and the 2 percent RMS requirement for the variation of the delivered cell efficiencies.

2.4 Task 5: Verification R-O Cell Performance by National Renewable Energy Laboratories

The progress on this task has been delayed by the "work overload" at EMCORE and equipment problems at National Renewable Energy Laboratories (NREL). We have now received the R-O cells from EMCORE and the equipment problem (large area one simulator) at NREL has been resolved.

Arrangements have been made with Tom Moriarte at National Renewable Energy Laboratory (NREL) who will repeat the characterization of R-O cells at one- and 500 suns as described under Task 4 above. The time window is expected to be mid-September to Mid October.

Table 3: Distribution of Conversion Efficiency of Delivered Cells

| Percentage Bracket for Conversion Efficiency | Number of Cells Within Percentage Bracket | Percentage of Cells Within the Bracket |
|---|---|---|
| 36% | 2 | 0.95% |
| 37% | 193 | 91.90% |
| 38% | 15 | 7.15% |

2.4.1 United Innovations Task Objectives

- Test cell performance at one sun and 500 suns
- Measure Total, Specular, and Diffuse Reflectance from the top surface of the cells (a few representative cells)
- Determine the percentage coverage of the cell top surface by contact grid finger system
- Obtain Performance Plot for the Anti-Reflective Coating

2.4.2 Deliverables

 Report verifying manufacturer's performance claims to cover test results required under this task

2.5 Task 6: Design & Manufacture of an 8 x 8 Cell Photovoltaic Submodule of Triple Junction Resistivity-Optimized Cells

2.5.1 United Innovations Task Objectives

United Innovations will procure 15 Direct bonded Copper (CBC) substrates from Curamic Electronics.

United Innovations shall develop and provide Curamic Electronics with the with the copper circuitry design for the eight by eight sub-array including cell circuitry and the leads for by-pass diodes and blocking diodes which are going to be installed externally to the PVCC box. The cell array circuitry will consist of eight strings of cells in parallel, where each string will have eight cell connected in series. The nominal open circuit voltage of the sub-array will be slightly over 24 V. At nominal peak power output (1100W) with a 2.1 m dish the total current flowing through the array will be 45.83 Amps. Thus each string (and every cell in the string) will carry a nominal current of 5.73 Amps.

Curamic Electronics shall etch the copper circuitry provided by UI. The etched sub-arrays will be shipped to EMCORE to complete the mounting of the cells. The completed sub-arrays will be characterized at one sun and 500 sun concentration by NREL.

With the understanding of the Energy Commission Project Manager following necessary modifications were made to this task. a) United Innovations procured 10 etched and 4 unetched DBC substrates, b) Instead of a 2.1 m dish, University of Arizona provided UI with a 2.5 m dish. Thus the nominal power outputs and currents changed, respectively; a) Nominal peak power Output: 1,559W, b) Total Current: 64.94 Amp and c) String Current: 8.12 Amp and c) NxGen instead of EMCORE did perform the die-attaching of the cells onto the DBC substrates. EMCORE selected not to this task, d) for better monitoring purposes each individual string on the PV Sub-Module (8 cells in series) were independently connected to the external power terminals. Thus no internal Blocking Diodes were necessary.

2.5.2 United Innovations Task Objectives

- 1. Design appropriate copper circuitry for the 8 x 8 sub-array
- 2. Provide circuitry to Curamic Electronics
- 3. Manage and monitor the etching of the appropriate copper circuitry by Curamic Electronics
- 4. Provide sub-arrays to EMCORE for cell mounting
- 5. Manage and monitor the mounting of the R-O cells on the sub- array

2.5.3 Deliverables

Publicly available memorandum on the operating, eight cell by eight cell sub-module, consisting of resistivity optimized high-concentration cells, that includes a discussion that fully addresses the each of the following questions:

- Was a functioning sub-array produced?
- Did the sub-array satisfy the performance metrics?
- Was there test plan? If yes, what was it and was it successfully followed?
- If any, what were the barriers to producing a functioning sub-array?
- If any, how were the barriers to producing a functioning sub-array overcome?
- We are planning to overcome the problem by soldering the sub-array directly to the heat exchanger rather than using epoxies as we tried before.
- What is the time frame for market penetration of the sub-array?
- Who are the expected users of the sub-array?
- Who are the expected users of the sub-array?
- Were proprietary software, hardware, algorithms, and processes for optimization successful? If not what were the challenges and were they overcome?

2.5.4 Publicly Available Memorandum

As per workload difficulties at the EMCORE Plant UI received the Resistance optimized (R-O) cells late in August, 2010. The respective Photovoltaic Sub-Module that will use R-O cells is now under construction. However, to make the best possible use of time, UI designed, built and tested a prototype sub-array that uses Off-the-Shelf (S-O) cells. The substitution of R-O cells with S-O cells is perfectly adequate for addressing many of developmental issues that are

actually identical for both cell types. This is possible because the cells have exactly the same physical dimensions; they consist of the same material and have the same thermal characteristics. In virtue of these facts we will address the questions of Task 6 below based our experience with the fully assembled and tested O-S prototype. The results of the testing with the Photovoltaic Sub-Module using R-O cells will be included in the Final Report.

2.5.5 Production of the Functioning PV Submodule

Figure 16 shows the photo of the functioning prototype submodule.

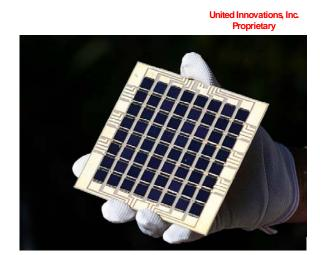


Figure 16: Fully Integrated 8 X 8 Cell Solar Submodule

Fully Manufactured 8 Cell by 8 Cell Solar Sub-Array

Figure 17 shows the circuitry patterning prepared for Curamic Electronics.

Figure 17: Circuitry Pattern and Critical Dimensions for the 8 X 8 Cell Photovoltaic Submodule on a 5" X 5" DBC Substrate

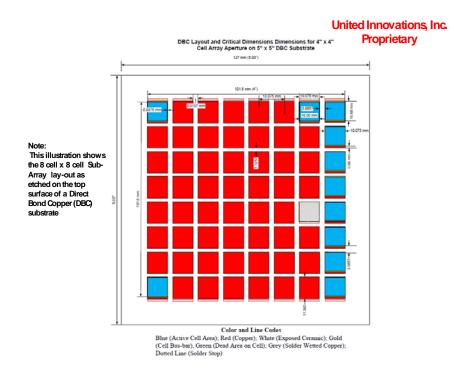


Figure 18: Rendering of the Etched Solar Sub-Array Layout on DBC Substrate

United Innovations, Inc.
Proprietary

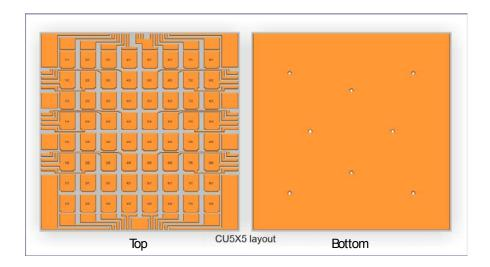
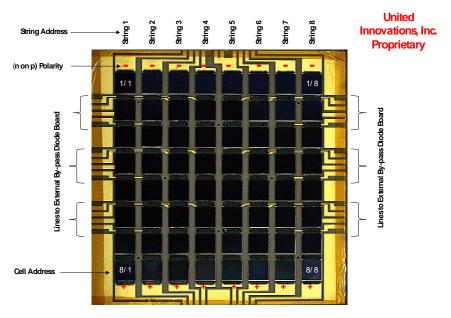


Figure 19 shows the cell and string addresses of the Photovoltaic Sub-Module ready to be installed.

Figure 19: Address Codes for the Cells and the Strings on the Actual Solar PV Submodule Subarray



Address Codes for Cells and Strings

Figure 20 shows the "one sun" test set-up of the Sub-Array after it was thermally bonded to the heat exchanger (a highly critical step). The measured VOC and ISC values for all Strings were in agreement with the expected one sun data reported by EMCORE. A Fluke 187 True RMS Multimeter was used to measure the Isc and the Voc values for all Strings.

Figure 20: One Sun Testing Photovoltaic Submodule to Validate the Functioning of the Unit



2.5.6 Satisfying the Performance Metrics: Photon Recycling and Conversion Efficiency

a) Photon Recycling Efficiency

The key performance metrics for this project is the photon recycling efficiency of the PVCC module. To quantify this very important parameter extensive outdoor experiment performed using the Tucson Test Facility and the parabolic dish shown in figures 32 through 37. The photon recycling efficiency can be measured just by measuring the Voc and Isc of each independent String by making subsequent measurements with and without the front lid of the PVCC. The ratio of the Isc x Voc products with- and without lid on provides photon recycling efficiency for the PVCC module. Unlike the conversion efficiency, the exact knowledge of the solar flux and that of the cell temperature is not necessary as long as these parameters stay constant during both experiments. For any relative changes in these parameters the data have to be normalized for the variation in solar flux and temperature. The data shown in Table 2 were taken with a FLUKE 187 True RMS Multimeter. Due to temperature instability and long duration of the experiments the temperature and flux data were normalized to each other and then normalized to standard 25 percent C operational temperature.

Table 4: Photon Recycling Data and Results

| String No. | Pon =Voc x Isc | Poff = Voc X Isc | Pon/Poff | Photo Recycling Eff. |
|------------|----------------|------------------|----------|----------------------|
| | [W] | [W] | | [%] |
| 1 | 28.91 | 18.58 | 1.55 | 55 |
| 2 | 27.95 | 17.76 | 1.57 | 57 |
| 3 | 29.01 | 18.51 | 1.57 | 57 |
| 4 | 26.84 | 16.33 | 1.64 | 64 |
| 5 | 26.76 | 17.73 | 1.51 | 51 |
| 6 | 27.53 | 20.88 | 1.32 | 32 |
| 7 | 25.54 | 16.94 | 1.51 | 51 |
| 8 | 25.11 | 16.10 | 1.56 | 56 |
| Total | 217.64 | 142.83 | 12.24 | 52 |
| , | 53 | | | |

b) Conversion Efficiency at Higher Concentrations

Outdoor experiments performed at the Tucson Test Facility have shown that thermal interface coupling between the DBC substrate and the top of the heat exchanger is not adequate to handle higher solar concentrations. Figure 21 is a cross-sectional schematic of this most critical interface

(bluish tinted zone on the schematic). Our in depth studies and experiments with thermal epoxy's and Transient Liquid Phase Sintering Adhesives did not result in a satisfactory solution. During the experiments the cell temperature rose and a stable condition to measure the efficiency accurately could not be achieved.

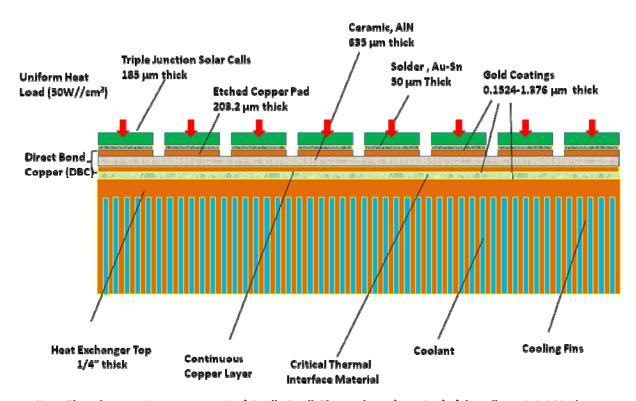
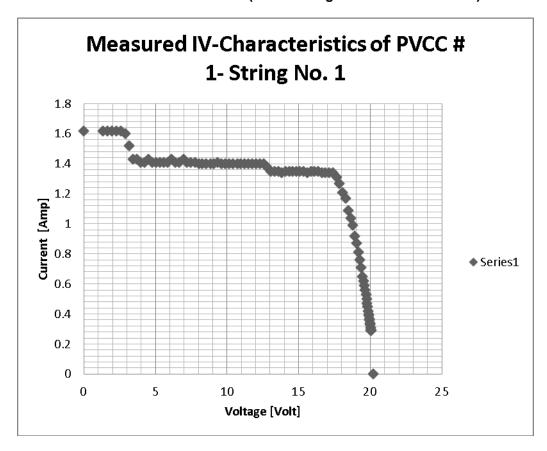


Figure 21: Cross-Sectional Schematic of the Water-Cooled Photovoltaic Submodule

Note: The solar array is a square matrix of 3 cell x 8 cell. The total area (top view) of the cell matrix is 16 inch square

For this reason we devised a method to be able to reduce the full solar flux density available (~700 suns) down to the levels (~200 suns). This was achieved by placing several layers of a wire mesh of known sun screening factor. Unfortunately this approach introduces strong flux non-uniformities at the plane of the solar cells within the cavity. This effect can be seen from the IV string characteristic plot shown on Figure 22. The sudden drop in current at about 3 volts is indicative that a by-pass diode was turned on due to strong flux uniformity across the string.

Figure 22: String I-V Plot Obtained With a SPIRE 800 Array Tester With Three Wire Meshes in Place (69.4W/String Available Solar Power)



The values Isc = 1.62Amp and Voc = 20.21 Volt do agree with the expected values. The measured Fill Factor (FFm) of 70 percent is lower than expected. However, the extrapolated Fill Factor (FFe) based on measured Isc = 1.62 Amp is 85 percent. Table 5 shows the calculated efficiencies for the respective FFm and FFe values.

Table 5: Preliminary Conversion Efficiency Results

| Available Solar Power /String [W] | Isc [Amp] | Voc [V] | Fill Factor [%] | String Cavity Eff. |
|--|-----------|---------|-----------------|--------------------|
| 64.4 | 1.62 | 20.21 | 70 | 35 % |
| 64.4 | 1.62 | 20.21 | 85 | 43.2% |
| Projected Cavity -String Conversion Efficiency | | | | > 35% |

The lower limit of 35 percent for the PVCC Cavity String Conversion Efficiency compares well with the highest HCPV module efficiency of 35 percent reported by Solar Australia, Pty. Our conversion efficiency result (>35 percent), although highly satisfactory, can only be considered

as an indication, rather than a conclusive result. These experiments shall be repeated under stable temperature conditions and accurate solar flux readings after elimination of the flux non-uniformity in the plane of the cells.

Test Plan and Its Success

The test plan was to build a complete PVCC receiver (see, Figure 22 through 31) and a special tracking Parabolic Dish and perform outdoor measurements of the system performance (see, Figures 32 through 37). As it can be seen from these figures and the results the test plan was successful.

Barriers in Producing a Functioning Submodule

There were no barriers with the Bub-Module prototype, however thermal coupling of the Sub-Module to the heat exchanger still requires further R&D as higher concentration levels cause the cells to overheat. At several hundred suns concentration the cell temperatures over 200C were recorded. Figure 22 shows the critical interface between the DBC and the heat exchanger.

Work to Be Done Overcome the Barriers

We are planning to overcome this barrier by using a pure indium based material called "Thermal Spring." This material is a micro-structured, thin sheet of indium manufactured by Induium Co. To facilitate the thermal coupling the sheet is sandwiched between DBC and the heat exchanger and the two parts are pressed against each other. This can be done by a set of screws at periodic distances. To reach metallic level thermal conductivities a continuous pressure of 40 PSI is needed.

Lead Time to Produce the Functioning PV Submodule

The manufacturing of cells was delayed at EMCORE because of their workload.

Cost of Manufacturing the Functioning Submodule

The cost of manufacturing the cells (not including testing and side experiments) was about \$65,000. This was close to our expectations

Time Frame for Market Penetration of the Submodule

Given the follow-up funding shown in Figure 35 we expect market entry b 2015

Market Path

At this demonstration phase we are planning to have a follow up stage to manufacture a full scale (40kW) turnkey Power Conversion Unit (PCU) unit that is geared towards commercialization. Next phase will involve the setup of a manufacturing plant for increased production volume (see, Figure 35).

Expected Users of the PV Submodule

The PV Sub-Module developed under this project will be packaged as a "turnkey" Power Conversion Unit (PCU) that consists of PVCC/Parabolic Dish/Tracking system/Inverter. The planned 40kW full scale PCU is designed for utility and stand alone distributed power plants.

Issues Regarding: Proprietary Software, Hardware, Algorithms, and Processes for Optimization We had no challenges regards proprietary software, hardware, algorithms, and process for optimization

CHAPTER 3: Photovoltaic Cavity Converter

As part of tour test plan to verify the Photovoltaic Sub-Module we designed and build a PVCC prototype. Below we briefly describe the key tasks we had in putting together a functional PVCC receiver that was used in the experiments.

3.1 Optical Design

Using the above described basic optical model we optimized the cavity dimensions to achieve the best possible flux distribution at the plane of the cells that are covering the rear cavity panel (see Figure 3). These data was used to create the CAD drawings to machine the mirrored walls (panels) of the PVCC Structure. Figure 23 shows the exploded view of the PVCC.

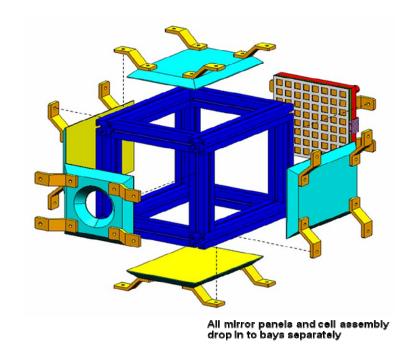


Figure 23: Exploded View of PVCC Showing the Mirrorized Front and Side Panels

3.2 Structural Design

To maintain flexibility and serviceability it was decided to construct the PVCC housing out of modular building "blocks". We used high precision aluminum extrusion bars for the frame and solid, but removable side walls. By using a shimming method we were able to align the PVCC to a large extend. The largest gap between the walls was kept below 1 mm. It was analytically determined that the light leakage was less than 8 percent, a value that can be improved upon. Figure 24 shows an oblique cross-cut of the fully assembled PVCC unit.

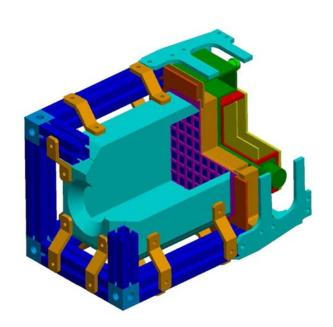


Figure 24: CAD Oblique Cross-Cut of the Fully Assembled PVCC

3.3 Heat Exchanger Design

Although it is possible to cool HCPV single cells (say, 10 mm x 10mm in size) with passive air convection, at high concentrations and large receiver areas (for example, 8 x 8 cell) it becomes necessary to use forced liquid cooling to remove the waste heat (~60 percent of total solar energy) from the Photovoltaic Sub-Module. The heat exchanger must also be designed with the worst possible scenario in mind such as, total conversion of the solar radiation into heat as no electric current can flow. At 500 suns this corresponds to heat load of ~50W/cm². Figure 25 shows the present design.

Figure 25: CAD Drawing of the Forced Water Heat Exchanger

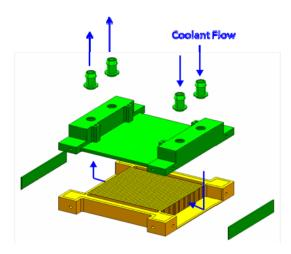
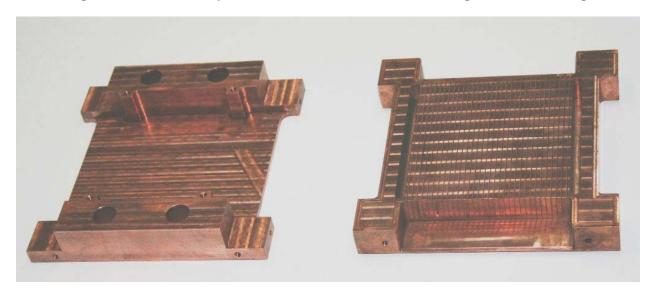


Figure 26 is the photo of the fully machined Heat Exchanger top and bottom. To avoid wear and tear and future leakages the top and bottom parts were integrated by high temperature brazing, rather than bolting and using a sealing gasket.

Figure 26: Machined Top and Bottom Parts of the Heat Exchanger Prior to Brazing



3.4 Manufacture and Assembly of PVCC Unit

Figure 27 shows the "rear-end" assembly from top to bottom): Mirror Mask, Flex Circuitry Photovoltaic Sub-Module, and the heat exchanger.

Figure 27: Photo of PVCC "Rear End" Assembly

United innovations, inc. Proprietary



Figures 28 through 29 show the sequences of the PVCC assembly steps.

Figure 28: "Rear Assembly" as Integrated Into the PVCC Housing

United Innovations Proprietary

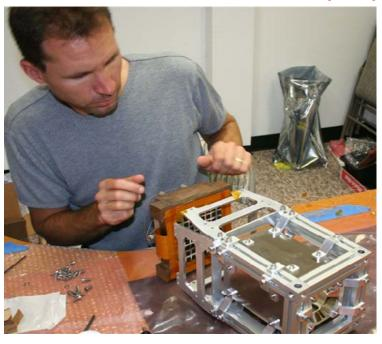


Figure 29: Junction Box Containing the Bypass Diode Board Is Being Attached to the Heat Exchanger

United innovations, inc. Proprietary

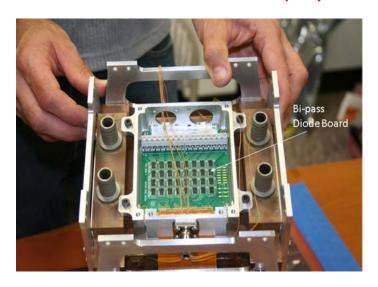


Figure 30: Photo of PVCC Showing the Front Panel With the Cavity Aperture

United Innovations, Inc.
Proprietary

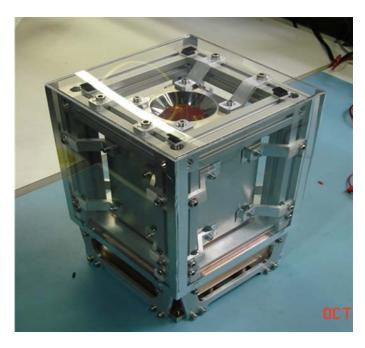


Figure 31: PVCC :Back Plate- Attachment Platform to Interface With the Dish

United Innovations, Inc. Proprietary

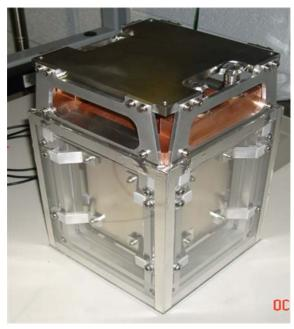
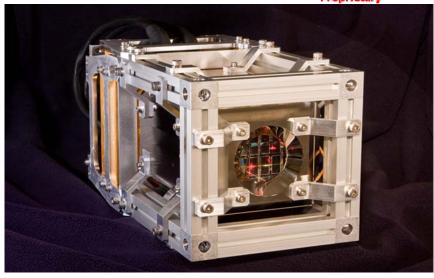


Figure 32: Photo of Test Ready PVCC Prototype



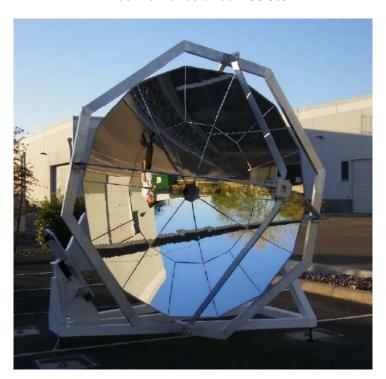


CHAPTER 4:Out-Door Test Facility

4.1 Parabolic Dish

Figure 33 shows the Tucson Embedded Systems (TES) Solar Facility that was built by TES in Tucson Arizona in association with this project. The 2.5 meter dish (f# 0.6) was designed and built by the University of Arizona. The support structure, the tracking and integration of the Dish/Tracker System was done by Raytheon. The funding was provided by Science Foundation Arizona and Raytheon under the Phase I using S-O cells.

Figure 33: All-Glass, Parabolic Dish Designed and Built by University of Arizona in Conjunction With This Project: Diameter = 2.5m, F-Number = 0.6, Back-Surface Mirror, Effective Reflectance = 88.5%



4.2 Tracking System

Figure 34: Support Structure and Sun-Tracking System Designed and Integrated by Raytheon in Conjunction With This Project



Figure 35: Outdoors Solar Test Facility Built and Operated by Tucson Embedded Systems



4.3 PVCC/Dish Assembly and Operation







Figure 37: Photo Showing Installed PVCC Provided With Cooling and Power Lines



Figure 38: PVCC Tracking the Sun at 700 Suns Concentration (Thermal Test)



CHAPTER 5: Summary of Project Stage and Recommendations

Photon Recycling, such as, "lid on" mode of operation improved the PVCC module conversion efficiency by 53 percent when compared to the no cavity, such as, "lid-off" mode of operation. This compares very well to the theoretically achievable limit of 61.3 percent. As per the key goal of this project (optimum recycling efficiency) 53 percent improvement is considered to be a success.

Preliminary experiments indicate that the PVCC module conversion efficiency could be between 35 to 43 percent. This is already above the highest module efficiency reported as of today (Solar Systems Australia, 35 percent).

Design and manufacture of the Resistivity optimized (R-O) cells has been completed successfully. 95 percent of the 210 cells received from EMCORE have a conversion efficiency of 37 percent when operating under 500 suns.

Several prototypes of 8 x 8 cells Photovoltaic Sub-Module's have been manufactured and tested successfully for electric operation and performance under one sun.

The lead-free, high temp "die-attach" process of the cells onto the Direct Bond Copper (DBC) substrates and their gold wire-bond interconnects have been proven to be successful (such as, strong bond and nearly void free).

The Photovoltaic Sub-Module copper circuitry on the DBC, including the by-pass diode lead has been designed and successfully etched.

To perform the process summarized above, the following side developments were simultaneously conducted. These were:

- A complete PVCC housing was designed build and tested. The major tasks involved were: Optical design and construction of the PVCC cavity, Thermal Management System of the Photovoltaic Sub-Module, External Electric Circuitry including By-pass Diode Board, Junction Box and the Field Connection Cables and so forth
- Establishment of an Outdoors Solar Test Facility including: A 2.5 m diameter, all glass parabolic dish (f# = 0.6) and associated Support Structure, Solar Tracking System, External Cooling System, Data recording system and an IV-tester.

There are some major challenges left that have to be resolved to be able to perform the ultimate efficiency testing of the R-O based PVCC Modules. These are:

• Development of a thermal coupling process between the Photovoltaic Sub-Module substrate (DBC) and the heat exchanger top surface. The requirements are: a) better than 40 W/mK thermal conductivity, b) 100 percent reliable and repeatable, c) insensitive to thermal fluctuations, and d) long life.

- A Temperature Monitoring System that provides uninterrupted temperature reading for each Cell and By-pass Diode
- Providing every cell on the PV Sub-Module with a By-pass Diode instead of every two
 cells as in the present design.
- A Solar Flux Measurement System that provides info on the exact amount of radiation entering the aperture of the PVCC and solar flux distribution in the plane of the cells.
- A fast, cooled shutter system in front of the PVCC aperture to allow "Pulsed" outdoor testing capability

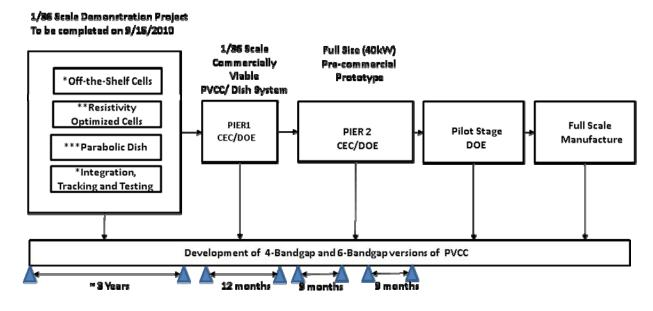
5.1 Recommendations

It is strongly recommended that the uninterrupted development of the PVCC/Dish systems continue with follow-up funding from the Energy Commission and the Department of Energy (DOE) to reach the Pilot Plant Stage (Pre-commercial full scale proto-type) and the Full Scale Manufacture for market entry (see Figure 38).

It is important to note that the "Resistivity Optimized Cell" stage of this project does not represent and "end phase" in the development of the PVCC/Dish Systems. As indicated in Figure 38 the PVCC systems provide a unique opportunity to develop 4-Bandgap and 6-Bandgap systems to achieve PVCC module efficiencies over 50 percent without the present multi-junction cell material limitations and the manufacturing difficulties.

Figure 39: Project Technology Road Map for a Successful Market Entry by 2015

United Innovations – Strategic Partner High Concentration PV Technology Road Map



Note: Time Scale not Continuous and not Linear

- * Funded by Raytheon (RMS)
- ** Funded by EJSG/CEC
- *** Funded by Science Foundation Arizona

GLOSSARY

| COE | Cavity Optical Efficiency |
|------|--|
| CPR | ?? |
| CTJ | Triple Function Cells |
| DBC | ?? |
| DOE | Department of Energy |
| HCPV | High Concentration Photovoltaic |
| LCOE | Levelized Cost of Electricity |
| NREL | National Renewable Energy Laboratories |
| NREL | ?? |
| OCE | Optical Cavity Efficiency |
| O-S | Off The Shelf |
| PCU | Power Conversion Unit |
| PV | Photovoltaic |
| PVCC | Photovoltaic Cavity Converter |
| R-O | Resistivity Optimized |
| TBD | To Be Determined |
| TES | Tucson Embedded Systems |